Received: 9 October 2024 | Revised: 12 December 2024 | Accepted: 28 December 2024

DOI: 10.1002/ardp.202400795

ARCH PHARM DPhG
Archiv der Pharmazie

FULL PAPER

Synthesis of new dihydropyrimidine derivatives and investigation of their antimicrobial and DNA gyrase inhibitory activities

Asaf Evrim Evren[1,2] | Demokrat Nuha[1,3] | Sam Dawbaa[1,4,5] | Uğur Kayış[6] | Ülküye Dudu Gül[7] | Leyla Yurttaş[1]

[1]Department of Pharmaceutical Chemistry, Faculty of Pharmacy, Anadolu University, Eskişehir, Turkey

[2]Department of Pharmacy Services, Vocational School of Health Services, Bilecik Şeyh Edebali University, Bilecik, Turkey

[3]Faculty of Pharmacy, University for Business and Technology, Prishtina, Kosovo

[4]Department of Pharmacy, Faculty of Medical Sciences, Thamar University, Dhamar, Yemen

[5]Department of Pharmacy, Faculty of Medical Sciences, Al-Hikma University, Dhamar, Yemen

[6]Department of Pharmacy Services, Pazaryeri Vocational School of Health, Bilecik Şeyh Edebali University, Pazaryeri, Bilecik, Turkey

[7]Department of Bioengineering, Faculty of Engineering, Bilecik Şeyh Edebali University, Bilecik, Turkey

Correspondence
Demokrat Nuha, Faculty of Pharmacy, University for Business and Technology, Prishtina, Kosovo.
Email: demokratnuha@gmail.com and demokrat.nuha@ubt-uni.net

Leyla Yurttaş, Department of Pharmaceutical Chemistry, Faculty of Pharmacy, Anadolu University, 26470 Eskişehir, Turkey.
Email: lyurttas@anadolu.edu.tr

Funding information
Anadolu University Scientific Research Projects, Grant/Award Number: 2204S036 (2100)

Abstract

Quinolone antibiotics are known for their antibacterial activity by inhibiting the enzyme DNA gyrase. Inspired by their mechanism, new compounds combining 1,4-dihydropyrimidine, a quinolone isostere, with pyridine/pyrimidine rings were synthesized. These derivatives showed antibacterial effects, likely through DNA gyrase inhibition, as supported by molecular docking and dynamics simulations. The synthesized compounds, 2-[(5-cyano-6-oxo-6-(pyridin-4-yl)-1,6-dihydropyrimidin-2-yl]-*N*-(benzothiazol-2-yl)-acetamide (**5a–5g**) and 2-[(5-cyano-6-oxo-6-(pyridin-4-yl)-1,6-dihydropyrimidin-2-yl)thio]-*N*-(thiazol-2-yl)acetamide (**6a–6f**), were evaluated for antibacterial activity. Compounds **5a**, **6b**, and **6c** demonstrated significant bactericidal effects. Against *Escherichia coli*, compounds **6b** and **6c** exhibited minimum inhibitory concentration (MIC) values of 1.95 and 0.97 µg/mL, respectively, comparable to the standard drug. Compound **5a** also showed strong activity against *Escherichia faecalis*. DNA gyrase inhibition studies confirmed that **5a**, **6b**, and **6c** inhibit the enzyme, as no supercoiled DNA band was observed. These findings highlight the potential of these compounds as antibacterial agents. Future development could focus on optimizing these structures for enhanced activity, similar to quinolone antibiotics.

KEYWORDS

1,6-dihydropyrimidine, antimicrobial, DNA-gyrase inhibition, quinolone

1 | INTRODUCTION

Diseases caused by microorganisms are a significant global health concern due to their widespread prevalence and potential for transmission. Managing these diseases often incurs substantial costs, particularly in cases where contagiousness leads to outbreaks requiring extensive public health interventions.[1,2] Although most microbial diseases are treatable, they can be fatal depending on the type of pathogen involved, including Gram-positive or Gram-negative bacteria, aerobic or anaerobic bacteria, mycobacteria, yeasts, or molds. These diseases may occur in isolation or in combination with other conditions.[3,4] Treatment becomes particularly challenging in individuals with weakened immune systems, such as those undergoing chemotherapy, living with AIDS, suffering from lupus, or recovering from organ or bone marrow transplantation. Additionally, vulnerable populations, including the elderly, pregnant women, and infants, face increased difficulty in overcoming microbial diseases.[5–9] Another significant challenge is the emergence of resistance to antimicrobial agents over time, which further complicates treatment efforts.[4,10–12] Consequently, there is a continuous need for the development of new antimicrobial agents with broad-spectrum activity, enhanced efficacy, reduced side effects, and improved pharmacokinetic profiles.[13–16]

Among antimicrobial agents, quinolones are broad-spectrum antibiotics widely used in the treatment of infectious diseases caused by Gram-positive bacteria and anaerobic bacteria. These compounds have been utilized in clinical practice since the 1960s.[17,18] In addition to their established activity, newer quinolone derivatives have demonstrated efficacy against mycobacteria and various atypical bacteria. Quinolones are classified into first, second, third, and fourth generations based on their development history, chemical structure, and spectrum of activity. Second, third, and fourth-generation quinolones are commonly referred to as fluoroquinolones.[19] Quinolones exert their antibacterial effects by inhibiting DNA replication through the suppression of bacterial DNA gyrase (topoisomerase II) and topoisomerase IV enzymes. Specifically, most quinolone antibiotics act by targeting DNA gyrase and topoisomerase IV. DNA gyrase comprises two subunits, GyrA and GyrB, while topoisomerase IV consists of ParC and ParE subunits. Resistance to quinolones arises from mutations in these target genes. For instance, a single amino acid substitution in the GyrA subunit of *E. coli* can impede the binding of fluoroquinolones to bacterial DNA, thereby conferring drug resistance.[20,21]

The inhibition of DNA synthesis is a key mechanism of action for antimetabolites among anticancer drugs. Chemically, antimetabolites mimic the structure of nucleobases found in DNA, which consist of purine and pyrimidine rings as their fundamental scaffolds. Antimetabolites such as 5-fluorouracil, cytarabine, gemcitabine, and capecitabine contain pyrimidine rings, while compounds like fludarabine and cladribine feature purine rings (Figure 1). Additionally, quinolone

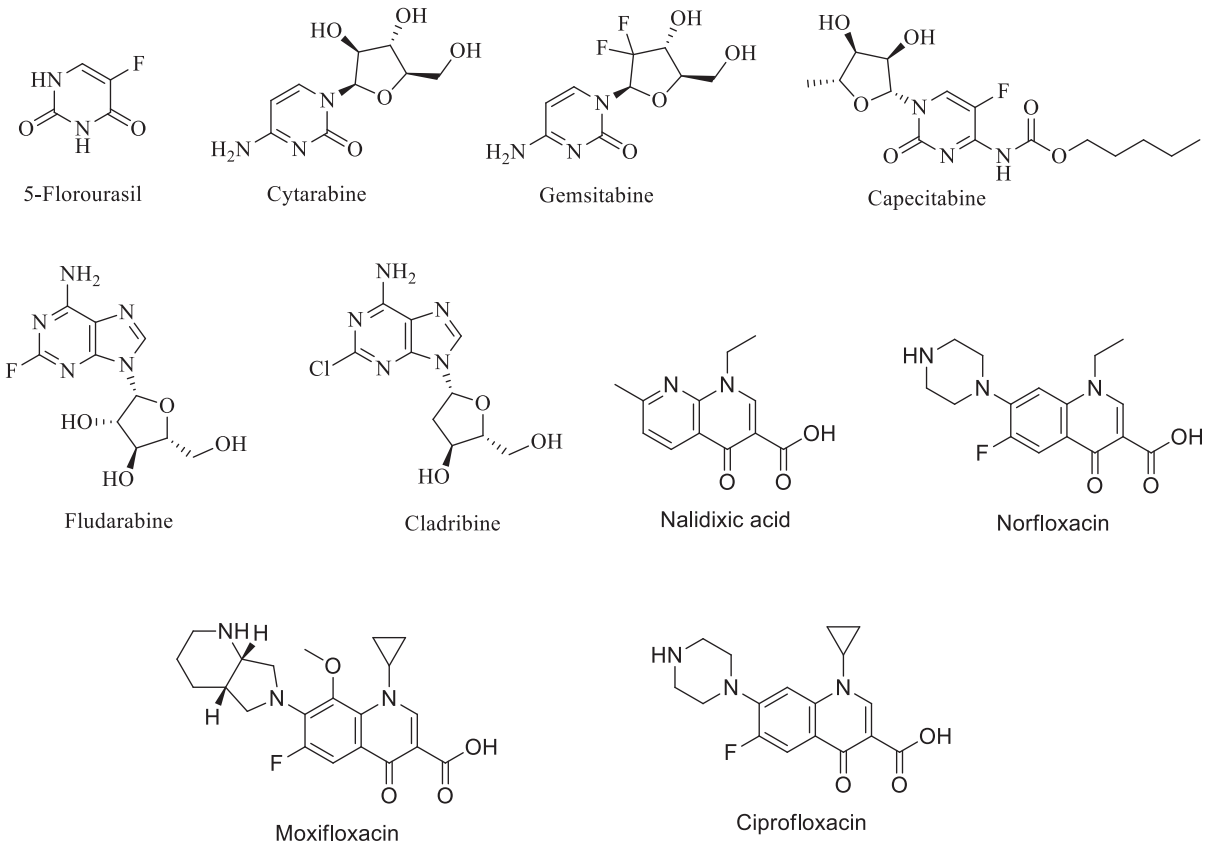

FIGURE 1 Antimetabolite anticancer drugs.

antibiotics, known for their antibacterial activity via inhibition of bacterial DNA gyrase, also share structural similarities with these antimetabolites. To provide a comprehensive comparative basis, we have included in Figure 1 the structures of key quinolone antibiotics such as nalidixic acid, norfloxacin, moxifloxacin, and ciprofloxacin. The inclusion of these compounds highlights their structural relevance to the study and supports the rationale behind synthesizing new derivatives that target bacterial and potentially tumor DNA synthesis.[22]

A diverse array of natural products and protein-based compounds have been identified and analyzed for their DNA gyrase inhibitory activity. Numerous chemical scaffolds have been characterized as promising candidates for the discovery of new antibacterial agents. Among these, quinolone and aminocoumarin have been established as core structures with DNA gyrase inhibitory properties.[23] Furthermore, in silico studies have demonstrated that chemical structures such as 2-amino triazine, 4-amino pyrimidine, 2-amino pyrimidine, and pyrrolopyrimidine exhibit DNA gyrase inhibitory effects.[24]

Despite the effectiveness of antimicrobial agents currently used in clinical practice, DNA gyrase inhibition remains a validated target for the development of novel antimicrobial drugs, particularly due to the increasing resistance to existing therapeutic regimens. Consequently, the synthesis of new gyrase inhibitors is a highly active area of research. In this study, 1,6-dihydropyrimidine-6-one derivatives were synthesized, drawing on the presence of the pyrimidine ring in antimetabolite anticancer drugs, the chemical structures of quinolones (which act as DNA gyrase inhibitors), literature data, and in silico studies. The antimicrobial properties and DNA gyrase inhibitory activities of the synthesized compounds were thoroughly evaluated.

2 | RESULTS AND DISCUSSION

2.1 | Chemistry

Targeted *N*-(benzothiazol-2-yl)-2-[5-cyano-6-oxo-4-(pyridin-4-yl)-1,6-dihydropyrimidin-2-yl]thio acetamide derivatives (**5a–5g**) and 2-{[5-cyano-6-oxo-4-(pyridin-4-yl)-1,6-dihydropyrimidin-2-yl]thio}-*N*-(thiazol-2-yl)acetamide derivatives (**6a–6f**). Method A was initially employed to yield 4-oxo-6-(pyridin-4-yl)-2-thioxo-1,6-dihydropyrimidin-5-carbonitrile (**1**). To obtain the desired 2-aminothiazole derivatives in the intermediate step, various α-halo ketones and thiourea were reacted with Hantzsch thiazole synthesis and proceeded according to Method B. The obtained substituted 2-amino thiazoles (**2**) and commercially available 2-amino benzothiazoles were acetylated with chloroacetyl chloride by Method C. The intermediates were characterized, and their melting points were determined. The final compounds were synthesized by reacting the pyrimidine derivative (1) with the acetylated thiazole/benzothiazole intermediates (**3**, **4**), according to Method D (Scheme 1). After purification of the synthesized result compounds, their structures were analyzed to elucidate their structures. The melting points of the compounds were determined and reaction yields were calculated. The compounds were obtained with yields between 67% and 79%. Structural characterization was performed using nuclear magnetic resonance (^{1}H-NMR, ^{13}C-NMR), and high-resolution mass spectrometry (HRMS). In the ^{1}H-NMR spectra, the proton methylene group attached to the sulfur atom resonated between 3.82 and 4.07 ppm and in the ^{13}C-NMR between 34.54 and 38.37 ppm. As for the protons in the aromatic region, in the derivative carrying nonsubstituted benzothiazole (**5a**), the protons connected to the carbon atom 6 (C-6) and carbon atom 5 (C-5) of the benzothiazole ring were observed as a triplet, while the proton at carbon atom 7 (C-7) of the benzothiazole ring was observed as a doublet in the highest field. The protons at carbon atom 3 (C-3) and carbon atom 5 (C-5) of the pyridine ring were observed as a doublet, the signal of the proton at the carbon atom 4 (C-4) position of benzothiazole was observed as a doublet, and the signals of the protons at the carbon atom 2 (C-2) and carbon atom 6 (C-6) position of the pyridine ring were observed as a doublet in the lowest field. In the derivatives containing a thiazole ring, protons belonging to methyl- and ethyl-containing derivatives were detected in the aliphatic region as expected. In the ^{13}C-NMR spectra of the compounds, the signals belonging to the pyridine ring were easily determined, the signal around 150 ppm belongs to the carbon atom 2 (C-2) and carbon atom 6 (C-6) position of the pyridine ring, and the signals at the 3.5 position belong to the carbon atom 3 (C-3) and carbon atom 5 (C-5) position. Other aliphatic and aromatic carbon signals were as expected. In the high-resolution mass spectra of the compounds, positive mode ions were detected, confirming the molecular weights.

2.2 | Biological activity results

2.2.1 | Antimicrobial activity

The antimicrobial activity of the synthesized compounds was evaluated using the microdilution technique to determine their minimum inhibitory concentration (MIC) values against a range of bacterial and fungal pathogens. The MIC values (μg/mL) of the compounds are presented in Table 1 and were compared with standard drugs: azithromycin for bacterial strains and voriconazole and fluconazole for fungal strains. Among the compounds tested, compounds **5a**, **6b**, and **6c** were identified as the most active, exhibiting strong antimicrobial effects.

Compound **6c** emerged as the most potent among the tested compounds, showing MIC values of 0.97 μg/mL against *E. coli* (ATCC 25922), 3.90 μg/mL against *Serratia marcescens* (ATCC 8100), and 15.625 μg/mL against *Candida albicans* (ATCC 24433). These MIC values were comparable to the standard drug azithromycin for *E. coli* and *S. marcescens*, indicating that **6c** has a strong potential for combating these bacterial strains. Furthermore, compound **6c** displayed effective antifungal activity, with its MIC against *C. albicans* being significantly lower than that of fluconazole, making it a promising candidate for treating fungal infections as well.

Compound **6b** also demonstrated considerable antimicrobial activity, with MIC values of 1.95 μg/mL against *E. coli* (ATCC 25922), 62.5 μg/mL against *Staphylococcus aureus* (ATCC 29213), and 62.5 μg/mL against *C. albicans* (ATCC 24433). While its activity against *S. aureus* was lower than that of azithromycin, compound **6b** still showed significant antibacterial effects against *E. coli*, which is a

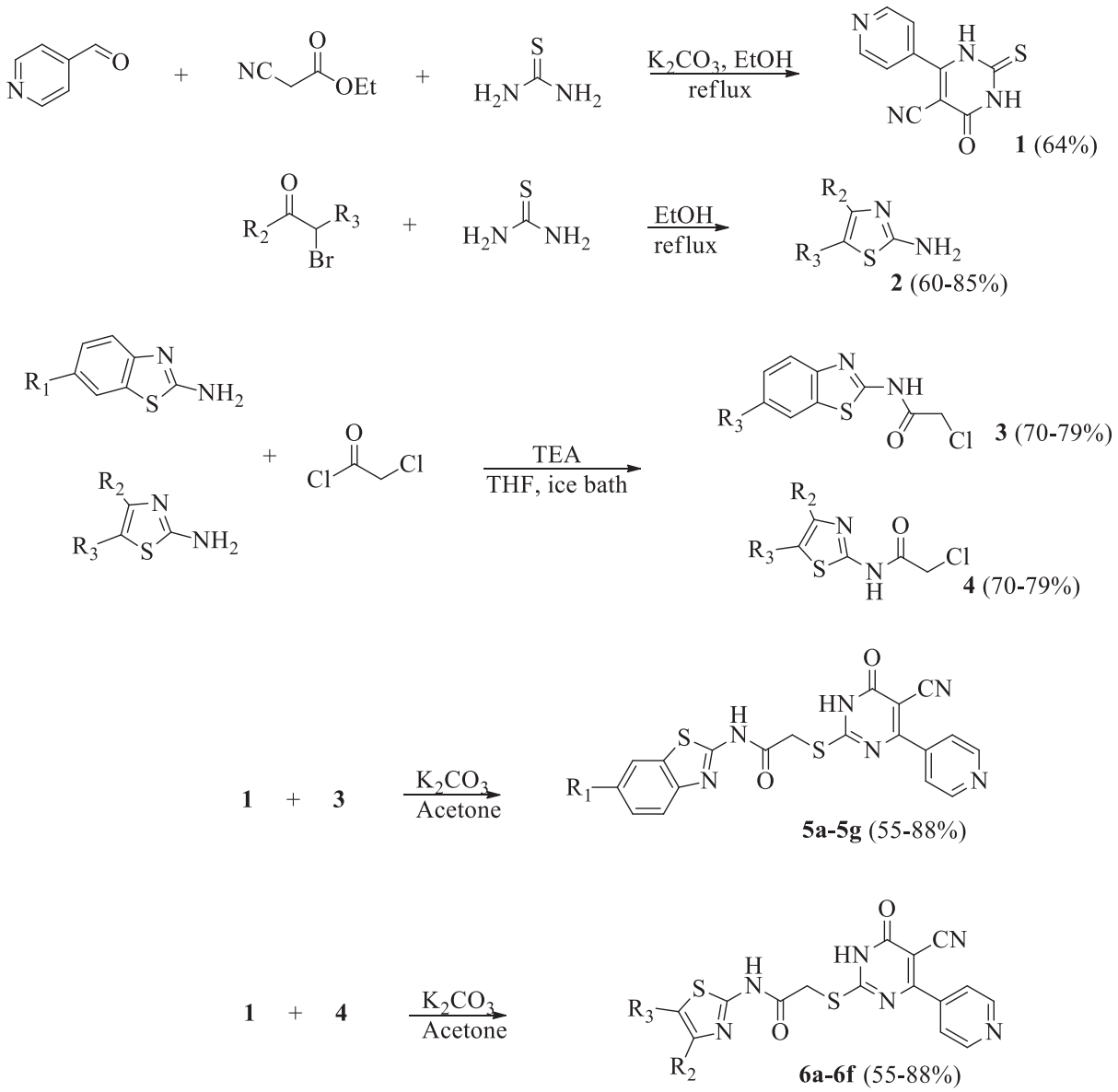

	R_1		R_2	R_3
5a	-H	**6a**	Ph	-H
5b	-F	**6b**	4-CNPh	-H
5c	-Cl	**6c**	4-NO_2Ph	-H
5d	-NO_2	**6d**	-H	-H
5e	-CH_3	**6e**	-CH_3	-COOEt
5f	-OCH_3	**6f**	-CH_3	-H
5g	-OCH_2CH_3			

SCHEME 1 Synthesis route of the target compounds (**5a–5g**, **6a–6f**).

common and problematic pathogen in both clinical and environmental settings. The activity against *C. albicans* was on par with that of the standard drug Voriconazole, highlighting the compound's potential for treating fungal infections.

Compound **5a** demonstrated noteworthy antimicrobial activity, particularly against *E. coli* (ATCC 25922), with a MIC value of 7.81 µg/mL. Additionally, compound **5a** exhibited significant antifungal activity against *C. albicans* with a MIC value of 3.90 µg/mL, comparable to the activity of voriconazole. Although its activity against *S. aureus* and *S. marcescens* was less pronounced compared with that of **6b** and **6c**, the high activity of **5a** against *E. coli* and *C. albicans* indicates its potential as a broad-spectrum antimicrobial agent.

When analyzing the activity of the compounds against other bacterial and fungal strains, it was found that none of the compounds were as effective as the standard drugs in certain cases. For instance, against *Pseudomonas aeruginosa* (ATCC 27853) and *Klebsiella*

TABLE 1 MIC values of the compounds against various microorganisms (μg/mL).

Com.	A	B	C	D	E	F	G	H	I	J	K	L
5a	15.625	62.5	62.5	125	<0.97	125	250	62.5	15.625	125	62.5	7.81
5b	15.625	62.5	62.5	125	15.625	125	250	15.625	31.25	125	250	15.625
5c	15.625	31.25	62.5	125	31.25	125	250	15.625	*3.90*	125	>250	125
5d	31.25	125	62.5	62.5	15.625	250	125	15.625	*3.90*	62.5	125	125
5e	15.625	62.5	125	125	7.81	125	250	15.625	7.81	125	250	125
5f	7.81	62.5	62.5	62.5	15.625	125	250	15.625	31.25	125	125	125
5g	7.81	62.5	125	62.5	62.5	250	125	7.81	62.5	125	125	7.81
6a	7.81	>250	62.5	125	3.90	>250	15.625	7.81	125	125	>250	125
6b	*1.95*	62.5	62.5	62.5	62.5	125	*1.95*	250	62.5	125	62.5	62.5
6c	*0.97*	31.25	62.5	15.625	*1.95*	15.625	3.90	62.5	62.5	62.5	62.5	31.25
6d	15.625	125	125	62.5	7.81	125	62.5	62.5	>250	125	125	125
6e	15.625	62.5	62.5	125	3.90	250	15.625	15.625	>250	125	>250	>250
6f	15.625	62.5	125	125	125	125	125	31.25	250	62.5	125	125
Azi	<0.97	<0.97	<0.97	<0.97	<0.97	<0.97	<0.97	<0.97	-	-	-	-
Vor	-	-	-	-	-	-	-	-	3.90	3.90	1.95	1.95
Flu	-	-	-	-	-	-	-	-	7.81	7.81	3.90	3.90

Note: Azi, standard Drug, Azithromycin; A, *Escherichia coli* (ATCC 25922); B, *Serratia marcescens* (ATCC 8100); C, *Klebsiella pneumoniae* (ATCC 13883); D, *Pseudomonas aeruginosa* (ATCC 27853); E, *Enterococcus faecalis* (ATCC 2942); F, *Bacillus subtilis*; G, *Staphylococcus aureus* (ATCC 29213); H, *Staphylococcus epidermidis* (ATCC 12228); I, *Candida albicans* (ATCC 24433); J, *Candida krusei* (ATCC 6258); K, *Candida parapsilopsis* (ATCC 22019); L, *Candida glabrata*; MIC, minimum inhibitory concentration; Vor, (Standard Drug 1), Voriconazole; Flu, (Standard Drug 2), Fluconazole; -, not tested; ---, not determined. Italicized values indicate compounds that exhibit the best activity among the tested samples.

pneumoniae (ATCC 13883), the compounds did not show MIC values as low as the standard drug azithromycin. However, the compounds exhibited varying degrees of effectiveness against other microorganisms, such as *Bacillus subtilis* and *Staphylococcus epidermidis*, with MIC values ranging from 7.81 to 250 μg/mL.

Among the fungal species, the compounds demonstrated moderate to strong activity against Candida glabrata, with compounds **5a** and **5g** showing the most significant inhibition. Compound **5c** exhibited antifungal activity similar to voriconazole against *C. albicans*, with MIC values of 31.25 and 125 μg/mL for other strains, suggesting that it has a broader antifungal spectrum. However, no significant activity was observed against *Candida krusei* and *Candida parapsilopsis*, where the MIC values for all compounds exceeded 250 μg/mL, indicating limited efficacy against these particular strains.

Overall, the results indicate that compounds **5a**, **6b**, and **6c** show excellent antibacterial and antifungal activities, comparable to or better than the standard drugs used in this study. These compounds, particularly **6c**, represent promising candidates for further development as antimicrobial agents. Their potential for inhibiting both bacterial and fungal pathogens, as demonstrated by their MIC values, suggests that they could be valuable in the treatment of infections caused by resistant strains. Further studies, including in vivo testing and the exploration of their pharmacokinetic properties, would be necessary to fully assess their therapeutic potential.

2.2.2 | DNA gyrase inhibition

Compounds **5a**, **6b**, and **6c**, which exhibited higher antimicrobial activity, were further evaluated for DNA gyrase inhibition. The study revealed that these compounds effectively inhibited DNA gyrase (Figure 2). No band corresponding to supercoiled DNA was observed. Therefore, it was concluded that the antibacterial activity of compounds **5a**, **6b**, and **6c** resulted from their inhibition of the DNA gyrase enzyme.

2.3 | In silico results

2.3.1 | ADME results

The five key physicochemical properties were assessed through an in silico ADME (Absorption, Distribution, Metabolism, and Excretion) analysis of compounds **5a–5g** and **6a–6f** using the SwissADME web-based software. Table 2 displays the computational prediction of the values for H-bond acceptor (HBA), H-bond donor (HBD), topologic polar surface area (TPSA), Log P, Log K, and the rule of 5. The target compounds have log P values between 1.27 and 2.85. The number of HBA was 6–8 and HBD was 2 by Lipinski's "Rule of 5" (HBD ≤5, HBA ≤10). TPSA values were calculated minimum as 117.96 $Å^3$ and maximum as 223.78 $Å^3$. Besides, log *Kp* values were predicted between

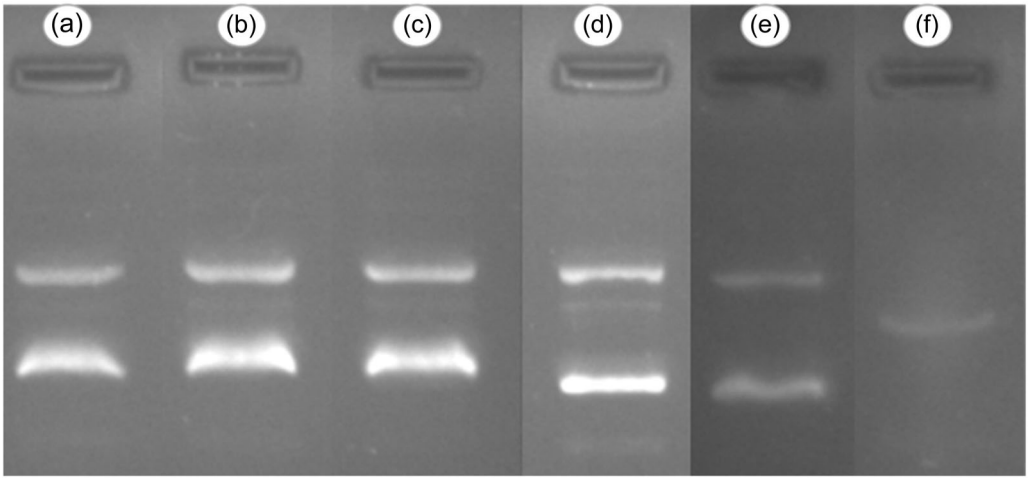

FIGURE 2 Visualization of the inhibitory effect of compounds **5a, 6b,** and **6c** and ciprofloxacin on *Escherichia coli* DNA gyrase by electrophoresis. (a) Compound **5a**: relaxed (pHOT) DNA, DNA gyrase and **5a** dissolved in dimethyl sulfoxide (DMSO); (b) Compound **6b**: relaxed (pHOT) DNA, DNA gyrase and **6b** dissolved in DMSO; (c) Compound **6c**: relaxed (pHOT) DNA, DNA gyrase and **6c** dissolved in DMSO; (d) Positive control: relax (pHOT) DNA, DNA gyrase and ciprofloxacin dissolved in DMSO; (e) Negative Control: relaxed (pHOT) DNA, DNA gyrase and DMSO only; (f) Linear DNA and DNA gyrase.

TABLE 2 Predicted ADME characteristics.

Com.	HBA	HBD	TPSA	Log *P*	Log *Kp*	Lipinski
5a	6	2	177.96	2.34	−7.15	Yes (0)
5b	7	2	177.96	2.59	−7.19	Yes (0)
5c	6	2	177.96	2.80	−6.92	Yes (0)
5d	8	2	223.78	1.46	−7.56	Yes (0)
5e	6	2	177.96	2.61	−6.98	Yes (0)
5f	7	2	187.19	2.28	−7.36	Yes (0)
5g	7	2	187.19	2.57	−7.19	Yes (0)
6a	6	2	177.96	2.55	−7.15	Yes (0)
6b	7	2	201.75	2.41	−7.50	Yes (0)
6c	8	2	223.78	1.89	−7.54	Yes (0)
6d	6	2	177.96	1.26	−7.86	Yes (0)
6e	8	2	204.26	1.96	−7.71	Yes (0)
6f	6	2	177.96	1.56	−7.67	Yes (0)

Abbreviations: HBA, H bond acceptor; HBD, H bond donor; Lipinski, Rule of Five (violation number); Log P, partition coefficient; Log K_p, skin permeation (cm/s); TPSA, topologic polar surface area (Å²).

−7.86 and −6.92. However, all compounds adhere to and satisfy the Lipinski rule, with all properties lying within a suitable range, according to their physicochemical properties.[25]

2.3.2 | Molecular docking

Following the identification of the active molecules (**5a**, **6b**, and **6c**), molecular docking studies were performed using the crystal structure of the DNA-DNA gyrase complex (PDB ID: 2XCT) (Figure 3). The results indicated that the compounds commonly chelate with manganese, with the 5-cyano-6-oxopyrimidine ring playing a crucial role in this interaction. Additionally, the aromatic rings of all three compounds, linked to the acetamide bridge, were observed to form π–cation interactions or aromatic hydrogen bonds with the Arg458 amino acid. The synthesized compounds were also found to engage in π–π stacking interactions with the DG: G9 nucleotide of DNA. These in silico interactions provide insights into the activity of the molecules and are consistent with the findings from both the literature[26,27] and in vitro enzyme assays. Furthermore, to better understand the stability of the ligand–protein complex over time and under varying environmental conditions, molecular dynamics simulation (MDS) was conducted for compound **6c**, as it exhibited a stronger inhibitory effect against *the E. coli* strain compared with the other two compounds.

2.3.3 | Molecular dynamics simulation studies

The docking pose of the 6c-DNA–DNA gyrase complex (PDB ID: 2XCT) was analyzed to gain a deeper understanding of the ligand–enzyme interactions. Based on the system stability plots (Figure 4a,bb), the radius of gyration (Rg) value of the ligand was calculated as 5.1 Å, while the maximum and minimum root mean square deviation (RMSD) values of the protein were within the acceptable range (1–3 Å). Specifically, throughout the simulation, the RMSD of the ligand relative to itself was 1.5 Å, and the RMSD of the ligand relative to the protein was 2.5 Å. Consequently, the RMSD peaks (Figure 4c) demonstrated consistent stability, with no significant fluctuations observed during the simulation period.

Additionally, the RMSF peaks were observed to remain below 1 Å when **6c** interacted with the enzyme's loop amino acids (the

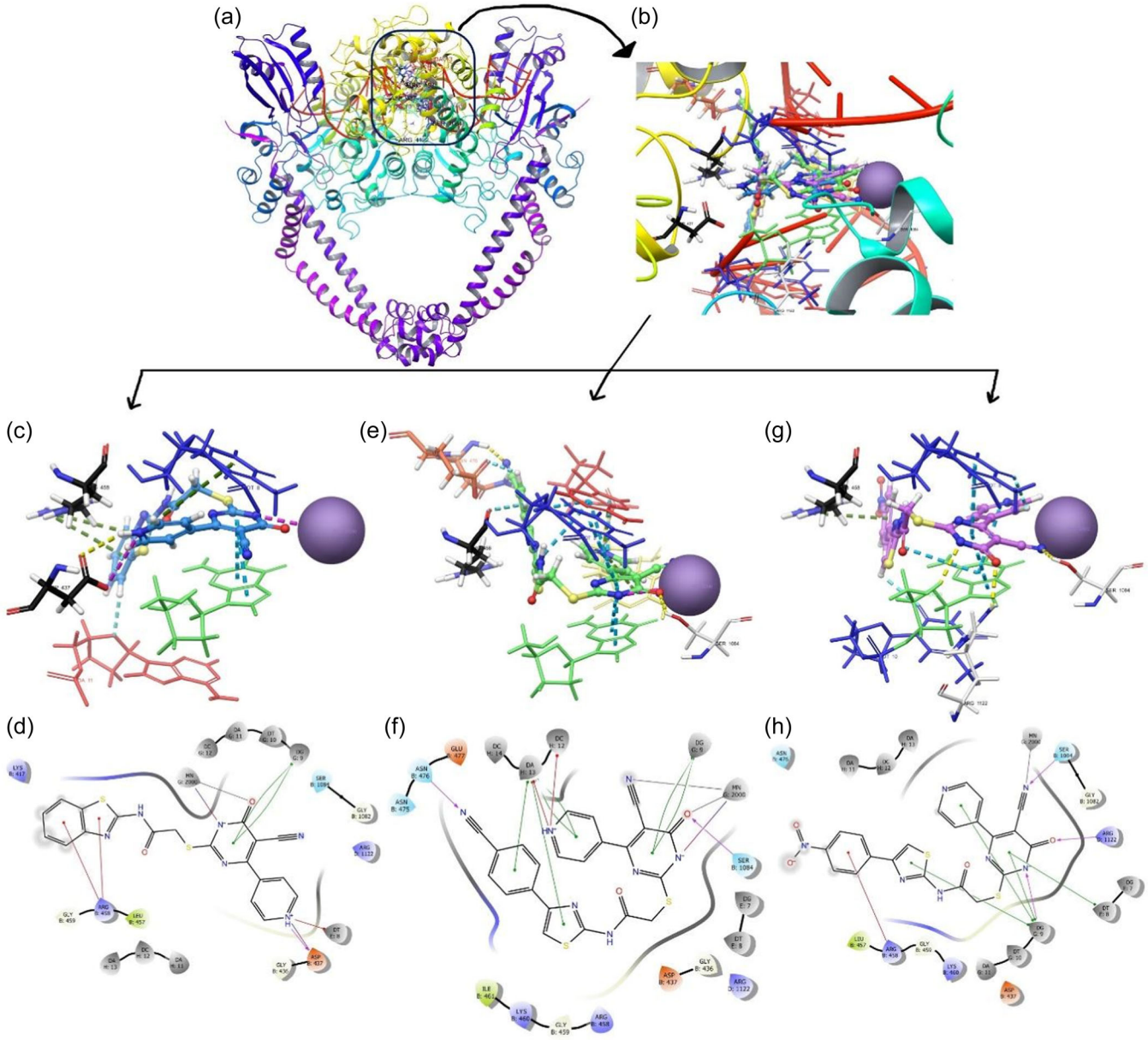

FIGURE 3 Interaction of active compounds with DNA and DNA gyrase and molecular docking results. (a) Image of the active site with DNA and DNA gyrase.(b) Zoomed three-dimensional (3D) image of active inhibitors superimposed in the enzyme active site.(c) and (d) 3D and two-dimensional (2D) pose for compound **5a**; (e) and (f) 3D and 2D pose for compound **6b;**(g) and (h) 3D and 2D pose for compound **6c**.

white area in the figure). These findings indicate that the stability of the complex was maintained throughout the simulation.

The MDS results (Figure 5a–c, and Supporting Information: Video [https://youtu.be/OqcY2KBR2Pw]) revealed that interactions with Arg458 (water-mediated hydrogen bonds and π–cation interactions), Lys460 (water-mediated hydrogen bonds), Ser1084 (hydrogen bonds), Glu1088 (water-mediated hydrogen bonds), and Arg1122 (hydrogen bonds) residues played a key role in binding. Notably, interactions with Arg1122 were consistently observed from the beginning to the end of the simulation. Furthermore, after 4.50 ns, interactions with Ser1084 became continuous, whereas the interaction fractions with Ser1085 and Glu1088 residues decreased.

Frequent interactions with DG:7, DT:8, DG:9, DC:12, and DA:13 nucleosides were also identified through π–π stacking. Additionally, **6c** formed hydrogen bonds with nucleic acids DG:9 and DA:13 while forming aromatic hydrogen bonds with DG:7, DT:8, DC:12, and DA:13. However, these interactions were less frequent than the π–π stacking interactions. The pyrimidine and 4-pyrimidone rings exhibited a strong affinity for the enzyme's binding pocket and nucleotides, whereas the thiazole moiety extended outside the active pocket, localizing between the DNA nucleotides.

To enhance DNA gyrase inhibition in future studies, replacing the cyano substitution with long-chain acidic derivatives, such as an acyl group, could be beneficial due to the observed loss of interactions with

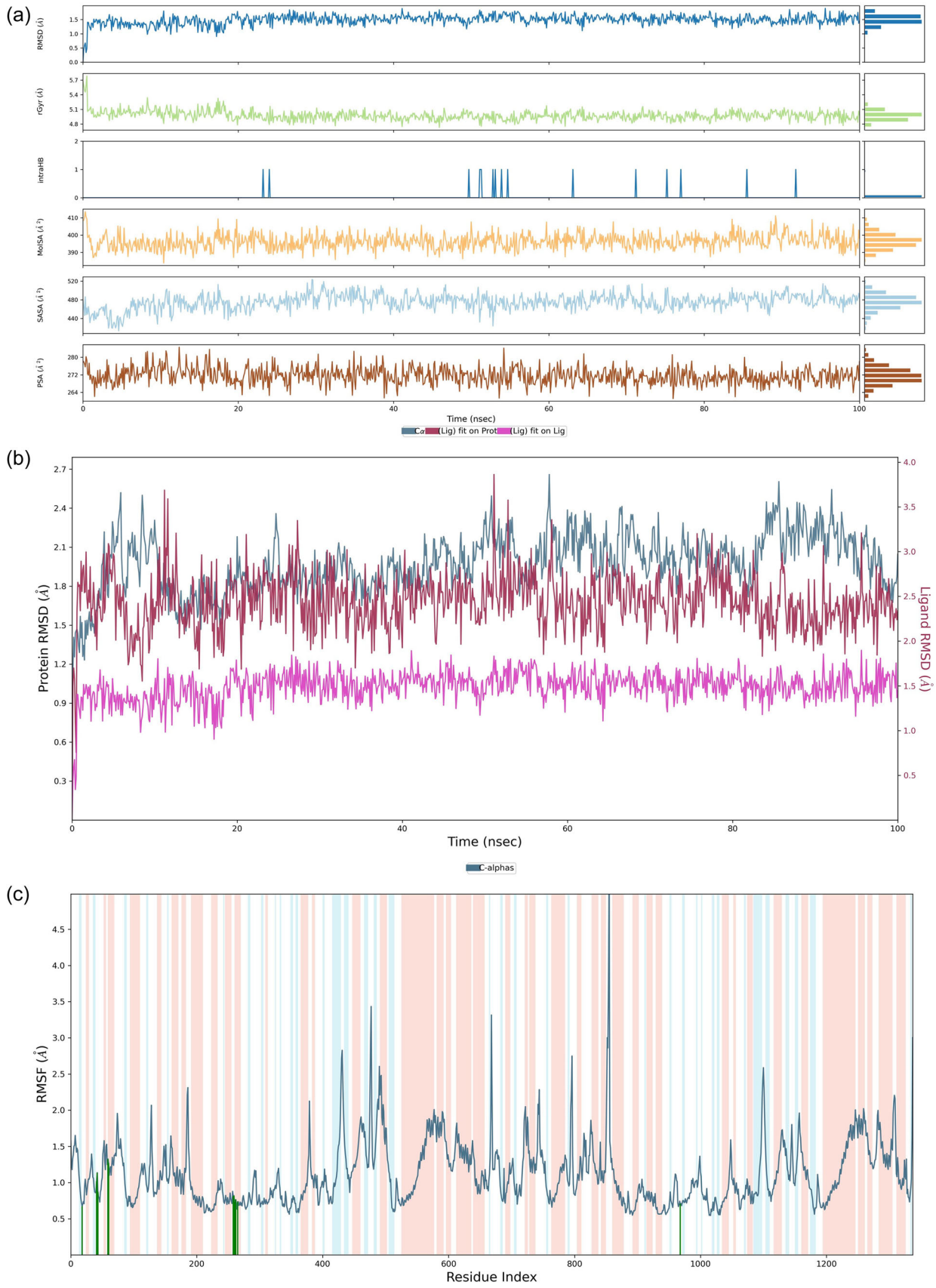

FIGURE 4 Stability plots of the molecular dynamics simulation (MDS) results for **6c**-DNA–DNA gyrase complexes. The stability properties (Rg, root-mean-square deviation (RMSD), and root-mean-square fluctuation (RMSF) plots, respectively) are shown in (a), (b), and (c) sections, respectively.

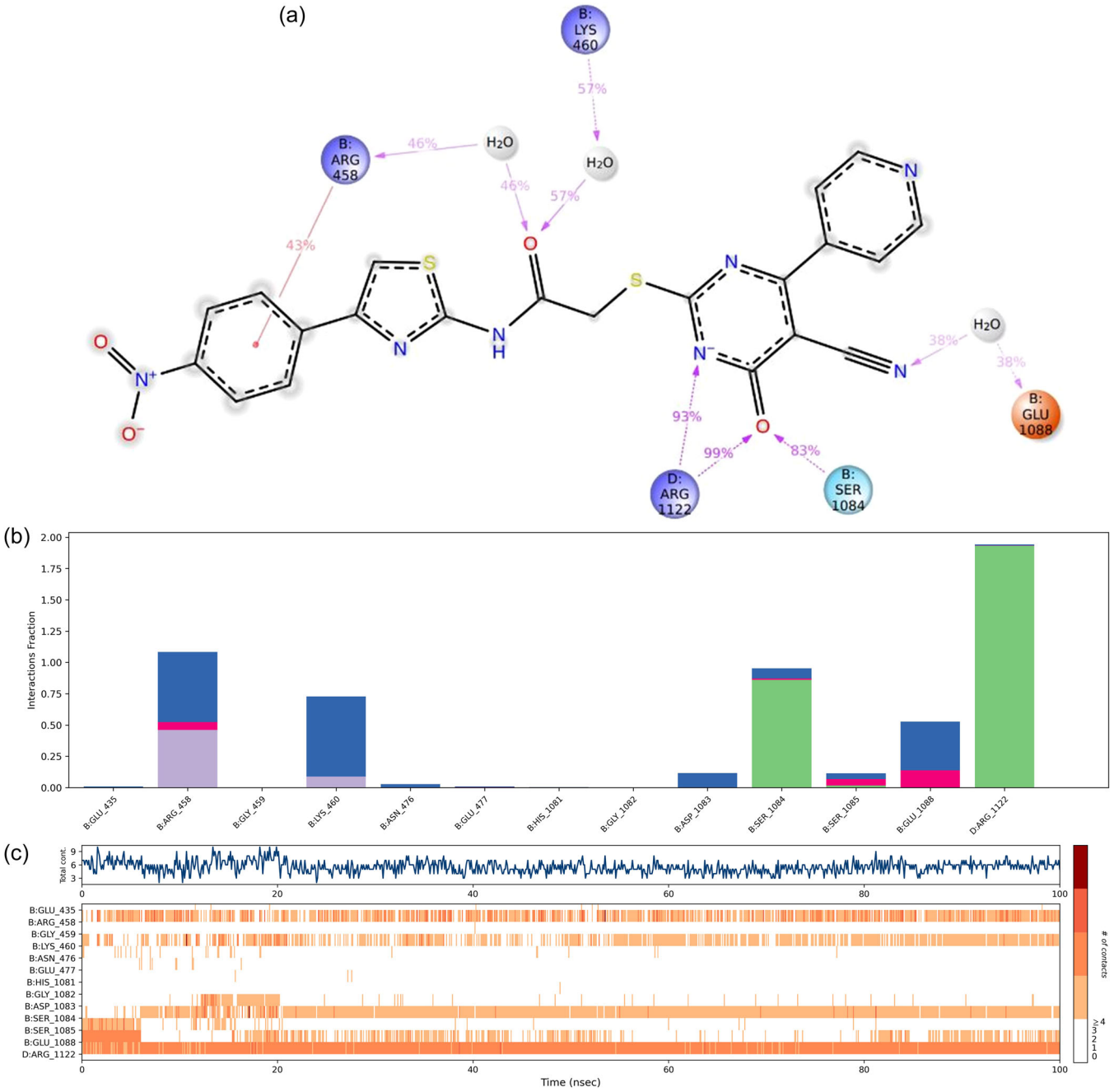

FIGURE 5 Interaction properties of the molecular dynamics simulation (MDS) result. (a) Two-dimensional (2D) interaction poses with connection strength (cutoff = 0.2) at the active region of DNA gyrase, (b) interaction fraction–residue diagram, and (c) number of interactions–interaction types–time plot for **6c**.

Glu1088 and Mn. The acetamide chain was identified as a crucial moiety, as it facilitated rotational flexibility within the active pocket.

The findings suggest that **6c** localized between the DNA and DNA gyrase enzyme, stabilizing itself through interactions with Arg458, Ser1084, Arg1122, DG:9, and DA:13 residues. Consequently, **6c** can be categorized as a DNA poison, similar to fluoroquinolone drugs. Its mechanism of action involves inhibiting the DNA gyrase enzyme.

In conclusion, both in vitro and in silico results demonstrated that linking 5-cyano-6-pyrimidinone and thiazole moieties with an acetamide bridge yields a compound with promising antimicrobial activity. This structure provides a valuable foundation for designing and synthesizing novel antimicrobial molecules targeting the DNA gyrase enzyme.

3 | CONCLUSION

Thirteen new 1,4-dihydropyrimidine derivatives (**5a–5g** and **6a–6f**) were synthesized based on the antibacterial effects of quinolone derivative antibiotics with DNA gyrase inhibitory properties. The derivatives with high antibacterial effects were tested for their DNA gyrase inhibitory

properties. A three-step synthesis procedure was used in the synthesis of the compounds. In the first step, 1,6-dihydropyridine intermediate was synthesized from ethyl cyanoacetate, thiourea, and pyridine-4-carboxaldehyde and then reacted with acetylated thiazole and benzothiazole derivatives to give the final compounds. The resulting compounds form two groups: thiazole carriers (**5a–5g**) and benzothiazole carriers (**6a–6f**). The structures of the resulting compounds, namely, *N*-(benzothiazol-2-yl)-2-[5-cyano-6-oxo-4-(pyridin-4-yl)-1,6-dihydropyrimidin-2-yl]thio acetamide (**5a–5g**) and 2-{[5-cyano-6-oxo-4-(pyridin-4-yl)-1,6-dihydropyrimidin-2-yl]thio}-*N*-(thiazol-2-yl)acetamide (**6a–6f**) derivatives, have been confirmed by spectroscopic techniques. Spectral analyses were carried out by proton and carbon nuclear magnetic resonance spectroscopy and high-resolution MS.

The antimicrobial activity of the compounds was evaluated against various Gram-positive and Gram-negative bacteria and fungi, and DNA gyrase inhibition was investigated for the three most active compounds: **5a**, **6b**, and **6c**. The compounds showed higher activity against Gram-negative bacteria, with *E. coli* being the most sensitive strain. Notably, compounds **6b** and **6c** demonstrated the highest inhibition against *E. coli*, with MIC values of 1.95 and 0.97 µg/mL, respectively, comparable to the standard drug azithromycin. Against Gram-positive bacteria, *E. faecalis* showed the highest sensitivity, with compound **5a** exhibiting the same MIC value (<0.97 µg/mL) as the standard. For fungi, *C. albicans* was the most sensitive strain, with compounds **5c** and **5d** showing antifungal activity comparable to the standard drug voriconazole, with MIC values of 3.90 µg/mL.

Additionally, thiazole-containing derivatives demonstrated superior activity compared with benzothiazole-containing ones. Compounds **5a**, **6b**, and **6c** effectively inhibited DNA gyrase, with in silico studies suggesting their localization between DNA and the DNA gyrase enzyme, stabilizing ligand–protein complexes. Molecular dynamics simulations clarified that those interactions between ligand parts and key residues—Arg458, Ser1084, Arg1122, DG:9, and DA:13—play a critical role in DNA gyrase inhibition.

4 | MATERIALS AND METHODS

4.1 | Chemistry

4.1.1 | General

All chemicals used in the syntheses were purchased either from Merck Chemicals (Merck KGaA) or Sigma-Aldrich Chemicals (Sigma-Aldrich Corp.). The reactions and the purities of the compounds were observed by thin layer chromatography (TLC) on silica gel 60 F_{254} aluminum sheets obtained from Merck. Melting points of the synthesized compounds were recorded by the MP90 digital melting point apparatus (Mettler Toledo) and were presented as uncorrected. ^{1}H NMR and ^{13}C NMR spectra (see the Supporting Information) were recorded by a Bruker 300 MHz and 75 MHz digital FT-NMR spectrometer (Bruker Bioscience) in dimethyl sulfoxide (DMSO)-d_6, respectively. In the NMR spectra, splitting patterns were designated as follows: s: singlet; d: doublet; t: triplet; m: multiplet. Coupling constants (*J*) were reported as Hertz. High-resolution mass spectrometric (HRMS) studies were performed using an liquid chromatography/mass spectrometry-ion trap-time of flight (LC/MS-IT-TOF) system (Shimadzu). Elemental analyses were performed on a Leco 932 CHNS analyzer (Leco).

The InChI codes of the investigated compounds are provided as Supporting Information.

4.1.2 | Synthesis of 2-mercapto-6-oxo-4-(pyridin-4-yl)-1,6-dihydropyrimidine-5-carbonitrile (**1**) (Method A)

4-Pyridinecarboxaldehyde (1 equivalent), ethyl cyanoacetate (1 equivalent), and thiourea (1 equivalent) were dissolved in ethanol, and K_2CO_3 (1.5 equivalent) was added. The mixture was boiled for 5–6 h with a magnetic heater under a reversible cooler. After the reaction was controlled by TLC, the crude product was removed by water treatment, dried, and crystallized from ethanol, resulting in a yield of 64%.

4.1.3 | Synthesis of thiazole-2-amine derivatives (**2**) (Method B)

Various α-halo ketones (1 equivalent) and thiourea (1 equivalent) were boiled in a flask with ethanol and stirred for 3–4 h. The end of the reaction was checked by TLC and the precipitate was filtered off, resulting in a yield of 60%–85%.

4.1.4 | General synthesis of *N*-(benzothiazol-2-yl)-2-chloroacetamide derivatives (**3**) and 2-chloro-*N*-(thiazol-2-yl)acetamide derivatives (**4**) (Method C)

After dissolving benzothiazole-2-amine derivatives or thiazole-2-amine derivatives (1 equivalent) in tetrahydrofuran, triethylamine (1.2 equivalent) was added and the mixture was brought to 0–5°C in an ice bath. 2-Chloroacetyl chloride (1.2 equivalent) diluted with tetrahydrofuran in a dropping flask was carefully added dropwise to the mixture, the solvent of the mixture was evaporated after stirring at room temperature for 2 h, and the raw material was washed with water and filtered, resulting in a yield of 70%–79%.

4.1.5 | Synthesis of *N*-(benzothiazol-2-yl)-2-{[5-cyano-6-oxo-4-(pyridin-4-yl)-1,6-dihydropyrimidin-2-yl]thio}acetamide (**5a–5g**) and 2-{[5-cyano-6-oxo-4-(pyridin-4-yl)-1,6-dihydropyrimidin-2-yl]thio}-*N*-(thiazol-2-yl)acetamide derivatives (**6a–6f**) (Method D)

N-(Benzothiazol-2-yl)-2-chloroacetamide derivatives (**2**) or 2-chloro-*N*-(thiazol-2-yl)acetamide derivatives (**4**) (1 equivalent) were stirred in acetone for 6 h at room temperature. K_2CO_3 (1.5 equivalent) was added as a catalyst. The end of the reaction was carried out by

controlling the TLC, and the solvent was allowed to volatilize. The resulting products were scraped off, and the raw material (**5a–5g** and **6a–6f**) was washed with water, filtered, and crystallized from ethanol, resulting in a yield of 55–88%.

N-(Benzothiazol-2-yl)-2-{[5-cyano-6-oxo-4-(pyridin-4-yl)-1,6-dihydropyrimidin-2-yl]thio}acetamide (**5a**): M.P.235–236°C, yield 68%, ^{1}H NMR (300 MHz, DMSO-d$_6$, ppm) δ 3.97 (s, 2H, S–CH$_2$), 7.16 (t, *J*:7.06 Hz, 1H, benzothiazole C$_6$-H), 7.32 (t, *J*:7.79 Hz, 1H, benzothiazole C$_5$-H), 7.61 (d, *J*: 8.04 Hz, 1H, benzothiazole C$_7$-H), 7.68 (d, *J*: 4.83 Hz, 2H, pyrimidine C$_{3,5}$-H), 7.82 (d, *J*:7.62 Hz, 1H, benzothiazole C$_4$-H), 8.60 (d, *J*: 4.83 Hz, 2H, pyrimidine C$_{2,6}$-H). ^{13}C NMR (75 MHz, DMSO-d$_6$, ppm) δ 36.59 (S–CH$_2$), 119.83, 120.03, 121.68, 122.47, 122.82, 125.72, 132.52, 145.18, 149.90, 150.18, 165.1, 158.55, 160.15, 170.31, 171.37, 172.79. HRMS (*m/z*): [M+1]$^+$ calculated $C_{19}H_{12}N_6O_2S_2$ 421.0536, found 421.0551.

N-(6-Florobenzothiazol-2-yl)-2-{[5-cyano-6-oxo-4-(pyridin-4-yl)-1,6-dihydropyrimidin-2-yl]thio}acetamide (**5b**): M.P.196–197°C, yield 70%, ^{1}H NMR (300 MHz, DMSO-d$_6$, ppm) δ 4.07 (s, 2H, S–CH$_2$), 7.27 (brs, 1H, benzothiazole C$_5$-H), 6.66–7.88 (m, 3H, Ar-H), 8.55 (brs, 2H, pyrimidine C$_{2,6}$-H), 8.70 (brs, 1H, Ar-H), 11.79 (brs, 1H, –NH). ^{13}C NMR (75 MHz, DMSO-d$_6$, ppm) δ 34.78 (S–CH$_2$), 108.41, 108.76, 114.45, 114.77, 118.67, 119.62, 122.00, 122.79, 133.11, 133.26, 145.04, 145.81, 150.13, 157.47, 158.55, 160.65, 162.66, 165.21, 169.29, 170.01, 171.98. HRMS (*m/z*): [M+1]$^+$ calculated $C_{19}H_{11}N_6O_2FS_2$ 439.0442, found 439.0454.

N-(6-Chlorobenzothiazol-2-yl)-2-{[5-cyano-6-oxo-4-(pyridin-4-yl)-1,6-dihydropyrimidin-2-yl]thio}acetamide (**5c**): M.P.240–241°C, yield 71%, ^{1}H NMR (300 MHz, DMSO-d$_6$, ppm) δ 3.93 (s, 2H, S–CH$_2$), 7.27 (d, H.8.17 Hz, 1H, benzothiazole C$_5$-H), 7.51 (d, *J*:9.19 Hz, 1H, benzothiazole C$_4$-H), 7.69 (d, *J*: 4.76 Hz, 2H, pyrimidine C$_{3,5}$-H), 7.83 (s, 1H, benzothiazole C$_7$-H), 8.63 (d, *J*:4.76 Hz, 2H, pyrimidine C$_{2,6}$-H). ^{13}C NMR (75 MHz, DMSO-d$_6$, ppm) δ 37.37 (S–CH$_2$), 119.85, 120.58, 120.95, 122.83, 124.80, 125.52, 125.63, 134.55, 145.22, 149.20, 150.20, 165.14, 170.56, 172.91, 173.12, 184.03. HRMS (*m/z*): [M+1]$^+$ calculated $C_{19}H_{11}N_6O_2ClS_2$ 455.0146, found 455.0157.

N-(6-Nitrobenzothiazol-2-yl)-2-{[5-cyano-6-oxo-4-(pyridin-4-yl)-1,6-dihydropyrimidin-2-yl]thio}acetamide (**5d**): M.P.223–224°C, yield 79%, ^{1}H NMR (300 MHz, DMSO-d$_6$, ppm) δ 3.96 (s, 2H, S–CH$_2$), 7.53 (d, *J*:8.47 Hz, 1H, Ar-H), 7.73 (s, 2H, Ar-H), 8.07–8.14 (m, 1H, Ar-H), 8.63–8.70 (m, 3H, Ar-H), 11.79 (brs, 1H, –NH). ^{13}C NMR (75 MHz, DMSO-d$_6$, ppm) δ 38.37 (S–CH$_2$), 117.63, 117.76, 118.13, 119.94, 121.13, 121.29, 122.84, 133.62, 140.70, 145.27, 150.24,157.08,165.09,170.70, 173.32, 174.00, 175.93. HRMS (*m/z*): [M+1]$^+$ calculated $C_{19}H_{11}N_7O_4S_2$ 466.0399, found 466.0387.

N-(6-Methylbenzothiazol-2-yl)-2-{[5-cyano-6-oxo-4-(pyridin-4-yl)-1,6-dihydropyrimidin-2-yl]thio}acetamide (**5e**): M.P.236–237°C, yield 69%, ^{1}H NMR (300 MHz, DMSO-d$_6$, ppm) δ 2.36 (s, 3H, CH$_3$), 3.90 (s, 2H, S–CH$_2$), 7.08 (d, 1H, *J*: 8.12 Hz, benzothiazole C$_5$-H), 7.42 (d, 1H, *J*: 8.12 Hz, benzothiazole C$_4$-H), 7.53 (s, 1H, benzothiazole C$_7$-H), 7.70 (d, *J*: 4.74 Hz, 2H, pyrimidine C$_{3,5}$-H), 8.64 (d, *J*: 4.74 Hz, 2H, pyrimidine C$_{2,6}$-H). ^{13}C NMR (75 MHz, DMSO-d$_6$, ppm) δ 21.47 (CH$_3$), 37.47 (S–CH$_2$), 89.59, 119.24, 119.89, 121.25, 122.83, 126.55, 130.85, 132.96, 145.26, 148.20, 150.20, 165.12, 170.53, 172.23, 173.23. HRMS (*m/z*): [M+1]$^+$ calculated $C_{20}H_{14}N_6O_2S_2$ 435.0692, found 435.0710.

N-(6-Methoxybenzothiazol-2-yl)-2-{[5-cyano-6-oxo-4-(pyridin-4-yl)-1,6-dihydropyrimidin-2-yl]thio}acetamide (**5f**): M.P.240–241°C, yield 67%, ^{1}H NMR (300 MHz, DMSO-d$_6$, ppm) δ 3.82 (s, 3H, OCH$_3$), 4.05 (s, 2H, S–CH$_2$), 7.03 (d, *J*: 8.65 Hz, 1H, benzothiazole C$_5$-H), 7.55–7.67 (m, 4H, benzothiazole C$_{4,7}$-H and pyrimidine C$_{3,5}$-H), 8.55 (d, *J*: 5.16 Hz, 2H, pyridine C$_{2,6}$-H), 12.39 (brs, 1H, –NH). ^{13}C NMR (75 MHz, DMSO-d$_6$, ppm) δ 34.72 (S–CH$_2$), 56.10 (OCH$_3$), 90.36, 105.20, 115.34, 119.63, 121.59, 122.52, 123.08, 133.26, 143.18, 145.06, 150.14, 156.44, 165.20, 168.84, 169.99, 172.00. HRMS (*m/z*): [M+1]$^+$ calculated $C_{20}H_{14}N_6O_3S_2$ 451.0642, found 451.0661.

N-(6-Ethoxybenzothiazol-2-yl)-2-{[5-cyano-6-oxo-4-(pyridin-4-yl)-1,6-dihydropyrimidin-2-yl]thio}acetamide (**5g**): M.P.201–202°C, yield 74%, ^{1}H NMR (300 MHz, DMSO-d$_6$, ppm) δ 1.35 (t, *J*: 6.73 Hz, 3H, CH$_3$), 4.03–4.08 (m, 4H, CH$_2$, CH$_2$ and S-CH$_2$), 7.02 (d, *J*: 8.64 Hz, benzothiazole C$_5$-H), 7.54 (s, 1H, benzothiazole C$_7$-H), 7.62–7.67 (m, 4H, Ar-H), 8.55 (d, *J*: 4.74 Hz, 2H, pyrimidine C$_{2,6}$-H), 12.41 (brs, 1H, –NH). ^{13}C NMR (75 MHz, DMSO-d$_6$, ppm) δ 15.17 (CH$_3$), 34.66 (S-CH$_2$), 64.06 (OCH$_2$), 105.86, 115.72, 119.64, 121.60, 122.80, 133.23, 143.08, 145.06, 150.13, 155.80, 156.27, 165.19, 168.76, 169.91, 171.95. HRMS (*m/z*): [M+1]$^+$ calculated $C_{21}H_{16}N_6O_3S_2$ 465.0798, found 465.0816.

2-{[5-Cyano-6-oxo-4-(pyridin-4-yl)-1,6-dihydropyrimidin-2-yl]thio}-*N*-(4-phenylthiazol-2-yl)acetamide (**6a**): M.P.220–221°C, yield 76%, ^{1}H NMR (300 MHz, DMSO-d$_6$, ppm) δ 4.02 (s, 2H, S–CH$_2$), 7.30–7.46 (m, 3H, Ar-H), 7.59 (s, 1H, thiazole C$_5$-H), 7.66 (d, *J*: 4.58 Hz, 2H, pyridine C$_{3,5}$-H), 7.90 (d, *J* = 6.10 Hz, 2H, Ar-H), 8.56 (d, *J* = 4.58 Hz, 2H, pyridine C$_{2,6}$-H), 12.44 (brs, 1H, -NH). ^{13}C NMR (75 MHz, DMSO-d$_6$, ppm) δ 34.73 (S–CH$_2$), 108.29, 119.69, 122.82, 126.13, 128.17, 128.90, 129.17, 134.85, 145.11, 149.26, 150.12, 165.12, 168.53, 169.95, 172.10. HRMS (*m/z*): [M+1]$^+$ calculated $C_{21}H_{14}N_6O_2S_2$ 447.0692, found 447.0702.

2-{[5-Cyano-6-oxo-4-(pyridin-4-yl)-1,6-dihydropyrimidin-2-yl]thio}-*N*-[4-(4-cyanophenyl)thiazol-2-yl]acetamide (**6b**): M.P.213–214°C, yield 71%, ^{1}H NMR (300 MHz, DMSO-d$_6$, ppm) δ 3.93 (s, 2H, S–CH$_2$), 7.65–7.70 (m, 3H, Ar-H), 7.82–7.85 (m, 2H, thiazole C$_5$-H, Ar-H), 8.06–8.09 (m, 2H, Ar-H), 8.62 (d, *J*: 4.07 Hz, 2H, pyridine C$_{3,5}$-H). ^{13}C NMR (75 MHz, DMSO-d$_6$, ppm) δ 36.59 (S–CH$_2$), 89.79, 109.58, 110.66, 119.60, 119.82, 122.83, 126.63, 133.02, 139.86, 145.21, 146.88, 150.18, 165.12, 170.42, 170.85, 172.96, 174.16. HRMS (*m/z*): [M+1]$^+$ calculated $C_{22}H_{13}N_7O_2S_2$ 472.0657, found 472.0645.

2-{[5-Cyano-6-oxo-4-(pyridin-4-yl)-1,6-dihydropyrimidin-2-yl]thio}-*N*-[4-(4-nitrophenyl)thiazol-2-yl]acetamide (6c): M.P.254–255°C, yield 75%, ^{1}H NMR (300 MHz, DMSO-d$_6$, ppm) δ 4.03 (s, 2H, S–CH$_2$), 7.66 (d, *J*: 5.41 Hz, 2H, pyrimidine C$_{3,5}$-H), 7.96 (s, H, thiazole C$_5$-H), 8.16 (d, *J* = 8.65 Hz, Ar-H), 8.31 (d, *J* = 8.33 Hz, Ar-H), 8.57 (d, *J*: 5.37 Hz, 2H, pyrimidine C$_{2,6}$-H), 12.63 (brs, H, -NH). ^{13}C NMR (75 MHz, DMSO-d$_6$, ppm) δ 34.92 (S–CH$_2$), 107.07, 119.68, 122.83, 124.46, 124.67, 126.74, 126.96, 145.10, 146.39, 146.85, 147.05, 148.28, 150.13, 165.15, 169.06, 170.00, 172.15. HRMS (*m/z*): [M+1]$^+$ calculated $C_{21}H_{13}N_7O_4S_2$ 492.0543, found 492.0546.

2-{[5-Cyano-6-oxo-4-(pyridin-4-yl)-1,6-dihydropyrimidin-2-yl] thio}-*N*-(thiazol-2-yl)acetamide (**6d**): M.P.190–191°C, yield 69%, ^{1}H NMR (300 MHz, DMSO-d_6, ppm) δ 3.37 (s, 2H, S–$\underline{CH_2}$), 7.19 (d, *J*: 3.47 Hz, thiazole C_5-H), 7.47 (d, *J*: 3.47 Hz, thiazole C_4-H), 7.65 (d, *J*: 4.29 Hz, 2H, pyrimidine $C_{3,5}$-H), 8.58 (d, *J*: 4.29 Hz, 2H, pyrimidine $C_{2,6}$-H), 12.20 (brs, 1H, -NH). ^{13}C NMR (75 MHz, DMSO-d_6, ppm) δ 34.58 (S–$\underline{CH_2}$), 90.27, 113.79, 116.73, 119.66, 122.80, 138.12, 150.16, 158.76, 165.15, 168.06, 169.99, 172.07. HRMS (*m/z*): $[M+1]^+$ calculated $C_{15}H_{10}N_6O_2S_2$ 371.0379, found 371.0396.

Ethyl 2-(2-{[5-cyano-4-oxo-6-(pyridin-4-yl)-1,4-dihydropyrimidin-2-yl]thio}acetamido)-4-methylthiazol-5-carboxylate (**6e**): M.P.243–244°C, yield 79%, ^{1}H NMR (300 MHz, DMSO-d_6, ppm) δ 1.23 (t, 3H, *J*: 7.40 Hz, $CH_2\underline{CH_3}$), 2.44 (s, 3H, CH_3), 3.82 (s, 2H, S–$\underline{CH_2}$), 4.13 (q, *J*:6.77 Hz, 3H, $\underline{CH_2}CH_3$), 7.70 (d, *J*: 4.54 Hz, 2H, pyrimidine $C_{3,5}$-H), 8.67 (d, *J*: 4.54 Hz, 2H, pyrimidine $C_{2,6}$-H). ^{13}C NMR (75 MHz, DMSO-d_6, ppm) δ 14.92 (CH_3), 18.11 (CH_3), 38.34 (S–$\underline{CH_2}$), 59.57 (CH_2), 120.01, 122.84, 145.35, 150.22, 157.42, 163.61, 165.03, 170.60, 173.57, 174.21. HRMS (*m/z*): $[M+1]^+$ calculated $C_{19}H_{16}N_6O4S_2$ 457.0747, found 457.0763.

2-{[5-Cyano-6-oxo-4-(pyridin-4-yl)-1,6-dihydropyrimidin-2-yl] thio}-*N*-(4-methylthiazol-2-yl)acetamide (**6f**): M.P.169–170°C, yield 76%, ^{1}H NMR (300 MHz, DMSO-d_6, ppm) δ 2.33 (s, 3H, CH_3), 3.97 (s, 2H, S–$\underline{CH_2}$), 7.12 (brs, 1H, thiazole C_5-H), 7.66 (d, 2H, pyrimidine $C_{3,5}$-H), 8.60 (brs, 2H, pyrimidine $C_{2,6}$-H).^{13}C NMR (75 MHz, DMSO-d_6, ppm) δ 11.61 (CH_3, 34.54 (S–$\underline{CH_2}$), 119.67, 121.17, 122.80, 126.49, 135.20, 145.06, 150.18, 156.97, 165.14, 167.77, 169.98, 172.08. HRMS (*m/z*): $[M+1]^+$ calculated $C_{16}H_{12}N_6O_2S_2$ 385.0536, found 385.0540.

4.2 | Biological activity studies

4.2.1 | Antimicrobial activity

The compounds were tested for antibacterial and antifungal activities against various Gram-negative, Gram-positive, and fungal species, and MIC_{90} values were determined. *E. coli* (ATCC 25922), *S. marcescens* (ATCC 8100), *K. pneumoniae* (ATCC 13883), *P. aeruginosa* (ATCC 27853), *E. faecalis* (ATCC 2942), *B. subtilis*, *S. aureus* (ATCC 29213), *S. epidermidis* (ATCC 12228) and fungi *C. albicans* (ATCC 24433), *C. krusei* (ATCC 6258), *C. parapsilopsis* (ATCC 22019), and *C. glabrata* (ATCC) were used as microorganisms. The Broth Microdilution procedure specified in the Clinical and Laboratory Standards Institute (CLSI) document M07-A9 was applied.[28] Bacterial cultures were obtained by incubating them overnight at 37°C in a Mueller–Hinton broth (MHB) medium. The turbidity of the inoculum (medium and microorganism) was adjusted to a Mac-Farland value of 0.5. The experiment was carried out by a twofold serial dilution technique. The well containing only microorganisms and medium and the well containing only medium were used as control wells. The presence and absence of growth in these wells, respectively, indicate the accuracy of the experiment and the absence of contamination. The compounds were diluted with 2% DMSO. The compounds were first applied at concentrations of 500 and 1.95 µg/mL. After application of the chemicals, the microplates were incubated at 37°C for 24 h. After the end of incubation, resazurin (20 µg/mL) was added to each well and incubated for another 2 h. At the end of the experiment, the microplates were read fluorometrically at 590 nm excitation and 560 nm emission values in a microplate reader, and MIC_{90} values were determined. The experiment was repeated twice for each chemical substance. For the anticandidal activity study, MIC_{90} values were determined against various *Candida* species. These values were obtained by performing experiments based on the EDef 7.1 document published by EUCAST.[29] *Candida* cultures were obtained by inoculating in RPMI medium and incubating at 37°C overnight. The inoculum turbidity of *Candida* species was adjusted to a Mac Farland value of 0.5, and the experiment was carried out with a two-fold serial dilution technique. The well containing only microorganisms and medium and the well containing only medium were used as control wells. The presence and absence of growth in these wells, respectively, indicate the accuracy of the experiment and the absence of contamination. The compounds were diluted with 2% dimethyl sulfoxide. The compounds were diluted from 500 to 1.95 µg/mL. After the chemicals were applied, the microplates were incubated at 37°C for 24 h. After incubation, resazurin (20 µg/mL) was added to each well and incubated for another 2 h. At the end of the experiment, the microplates were read fluorometrically at 590 nm excitation and 560 nm emission values in a microplate reader, and the MIC_{90} value was determined.

4.2.2 | Enzyme inhibition studies

The method for DNA gyrase assay inhibition was performed according to the kit protocol described by the supplier (SKU TG2000G-3, TopoGen). The assay buffer was prepared according to the formulation of 35 mM Tris30 Cl pH 7.5, 24 mM KCl, 4 mM $MgCl_2$, 2 mM dithiothreitol, 1.8 mM cypermidine, 1 mM ATP, 6.5% glycerol, and 0.1 mg bovine serum albumin (BSA)/mL. For each substance, 1 unit (U) DNA gyrase, five times the amount of assay buffer (4 µL) for 1U DNA gyrase, and 1 µL pHOT1 (Relax DNA) were added to the reaction medium. Finally, 10 µL of chemical substance(s) (ciprofloxazine, antimicrobial active compounds) were added to the experimental medium. Ciprofloxacin was used as a reference drug. All chemicals were added to the reaction medium according to their concentrations obtained as a result of antimicrobial activity (MIC_{90}), and the mixture was completed to 20 µL with water. After the mixture was incubated at 37°C for 1 h, 5 µL of stop buffer was added to the mixture, followed by 1 µL of proteinase K. The mixture was incubated again at 37°C for 30 min, and then, 20 µL of chloroform:isoamyl alcohol (24:1) was added and vortexed. Finally, the blue phase was removed and added to a 1% agarose gel with tris-acetate-EDTA buffer (TAE buffer) tetrahydrofuran. These procedures were followed for the three reaction media containing chemicals as well as for the mixture containing 1% dimethyl sulfoxide. As a positive control, media containing relaxed DNA and supercoiled DNA (relaxed DNA+DNA gyrase) were prepared and added to the agarose gel in the same

way. After all experiments were added to the gel, the electrophoresis method was applied by applying 1.5–2 V/cm electricity to the medium. When the mixture progressed to 80% of the gel, the gel was imaged with a molecular imaging device. This procedure was performed previously.[27]

4.3 | In silico studies

4.3.1 | ADME prediction

The essential physicochemical properties and pharmacokinetics of the final compounds (**5a–5g** and **6a–6f**) were predicted using the SwissADME web tool.[30] HBA, HBD, TPSA (Å^2), Log Po/w (consensus Log Po/w, the average of all five predictions), Log S (water solubility), GIA (gastrointestinal absorption), Log Kp (skin permeation (cm/s)), RoF (V) (Rule of Five violation number), and SA (synthetic accessibility) were predicted via in silico methods.

4.3.2 | Molecular docking studies

Molecular docking studies were performed to define the binding modes of the active compounds within the active regions of the DNA–DNA gyrase enzyme complex. The X-ray crystal structure (PDB ID: 2XCT) was retrieved from the Protein Data Bank server (www.pdb.org, accessed May 01, 2018). Schrödinger's Maestro interface and its applications (LigPrep,[31] and Glide modules[32]) were used for the molecular docking study. The applied procedure was performed in accordance with previously published works.[27]

4.3.3 | Molecular dynamics simulation studies

The MDS method is applied to predict the time-dependent stability of the active compound–protein complex. In this study, the methodology routine was performed as in reported studies.[27,33] In this study, the **6c**-DNA–DNA gyrase system (PDB ID: 2XCT) was investigated through 100 ns. Desmond's application of Schrodinger's Maestro[34] was used to achieve MDS results.

ACKNOWLEDGMENTS

The authors present their thanks to Anadolu University Scientific Research Projects for supporting this project. This research was funded by Anadolu University Scientific Research Projects under grant number 2204S036 (2100), and the APC was funded by Anadolu University. The MDS video can be watched via this link (https://youtu.be/OqcY2KBR2Pw).

Sample availability: Samples of the compounds **5a–5m** and **8a–8s** are available from the authors.

CONFLICTS OF INTEREST STATEMENT

The authors declare no conflicts of interest.

DATA AVAILABILITY STATEMENT

The data that support the findings of this study are available in the supplementary material of this article.

ORCID

Demokrat Nuha https://orcid.org/0000-0002-7271-6791
Sam Dawbaa http://orcid.org/0000-0001-7001-0739
Uğur Kayış http://orcid.org/0000-0003-0020-0857
Leyla Yurttaş http://orcid.org/0000-0002-0957-6044

REFERENCES

[1] J. Soni, S. Sinha, R. Pandey, *Front. Microbiol.* **2024**, *15*, 1370818.
[2] Z. F. Kapasi, *in* Acute Care Physical Therapy, Routledge, Taylor & Francis, New York, **2024**, pp. 149.
[3] P. Chakraborty, D. Chakraborty, *in* Essentials of Pharmacodynamics and Drug Action, Springer, Berlin, **2024**, pp. 169.
[4] A. Haider, M. Ikram, I. Shahzadi, M. Asif Raza, in *Polymeric Nanoparticles for Bovine Mastitis Treatment*, Springer, Cham, **2023**, pp. 81.
[5] P. S. Kurizky, L. L. dos Santos Neto, R. B. Aires, L. M. H. da Mota, C. M. Gomes, *Best Pract. Res. Clin. Rheumatol.* **2020**, *34*(4), 101509.
[6] T. H. Qin, J. C. Liu, J. Y. Zhang, L. X. Tang, Y. N. Ma, R. Yang, *Bioorg. Med. Chem. Lett.* **2022**, *72*, 128877. https://doi.org/10.1016/j.bmcl.2022.128877
[7] T. Zhu, X. Chen, C. Li, J. Tu, N. Liu, D. Xu, C. Sheng, *Eur. J. Med. Chem.* **2021**, *221*, 113524. https://doi.org/10.1016/j.ejmech.2021.113524
[8] M. Shafiei, L. Peyton, M. Hashemzadeh, A. Foroumadi, *Bioorg. Chem.* **2020**, *104*, 104240. https://doi.org/10.1016/j.bioorg.2020.104240
[9] R. Y. Shih, K. K. Koeller, *Radiographics* **2015**, *35*(4), 1141. https://doi.org/10.1148/rg.2015140317
[10] X. C. Yang, P. L. Zhang, K. V. Kumar, S. Li, R. X. Geng, C. H. Zhou, *Eur. J. Med. Chem.* **2022**, *232*, 114192. https://doi.org/10.1016/j.ejmech.2022.114192
[11] D. Osmaniye, A. Hıdır, B. N. Sağlık, S. Levent, Y. Özkay, Z. A. Kaplancıklı, *Chem. Biodiversity* **2022**, *19*, 8. https://doi.org/10.1002/cbdv.202200216
[12] N. R. Bandaru, P. Makam, P. Akshinthala, N. K. Katari, V. Banoth, B. Kolli, R. Gundla, *Molecules* **2022**, *27*(21), 7647. https://doi.org/10.3390/molecules27217647
[13] U. Acar Çevik, A. Işık, A. E. Evren, Ö. Kapusız, Ü. D. Gül, Y. Özkay, Z. A. Kaplancıklı, *SAR QSAR Environ. Res.* **2022**, *33*(11), 899. https://doi.org/10.1080/1062936X.2022.2149620
[14] N. F. Tay, M. Duran, İ. Kayagil, L. Yurttaş, G. Göger, F. Göger, F. Demirci, Ş. Demirayak, *Braz. J. Pharm. Sci.* **2022**, *58*, e191026.
[15] L. Senerovic, D. Opsenica, I. Moric, I. Aleksic, M. Spasic, B. Vasiljevic, *Adv. Exp. Med. Biol.* **2020**, *1282*, 37. https://doi.org/10.1007/5584_2019_428
[16] A. Y. Saiki, L. L. Shen, C. M. Chen, J. Baranowski, C. G. Lerner, *Antimicrob. Agents Chemother.* **1999**, *43*(7), 1574. https://doi.org/10.1128/AAC.43.7.1574
[17] D. C. Brittain, B. E. Scully, M. J. McElrath, R. Steinman, P. Labthavikul, H. C. Neu, *J. Clin. Pharmacol.* **1985**, *25*(2), 82. https://doi.org/10.1002/j.1552-4604.1985.tb02806.x
[18] D. Sriram, A. Aubry, P. Yogeeswari, L. M. Fisher, *Bioorg. Med. Chem. Lett.* **2006**, *16*(11), 2982. https://doi.org/10.1016/j.bmcl.2006.02.065
[19] R. C. Walker, *Mayo Clin. Proc.* **1999**, *74*(10), 1030. https://doi.org/10.4065/74.10.1030
[20] M. Wang, J. H. Tran, G. A. Jacoby, Y. Zhang, F. Wang, D. C. Hooper, *Antimicrob. Agents Chemother.* **2003**, *47*(7), 2242.
[21] X. Zhao, X. He, H. Li, J. Zhao, S. Huang, W. Liu, X. Wei, Y. Ding, Z. Wang, D. Zou, X. Wang, D. Dong, Z. Yang, X. Yan, L. Huang,

S. Du, J. Yuan, J. y Zhao, X. d Mu, Y. q Zhu, L. Xi, Z. Xiao, *FEMS Microbiol. Lett.* **2015**, *362*(18), fnv146.
[22] A. A. Wilde, in *Torsades de Pointes*, Elsevier, Amsterdam, **2022**, pp. 27.
[23] T. Khan, K. Sankhe, V. Suvarna, A. Sherje, K. Patel, B. Dravyakar, *Biomed. Pharmacother.* **2018**, *103*, 923. https://doi.org/10.1016/j.biopha.2018.04.021
[24] H.-J. Boehm, M. Boehringer, D. Bur, H. Gmuender, W. Huber, W. Klaus, D. Kostrewa, H. Kuehne, T. Luebbers, N. Meunier-Keller, F. Mueller, *J. Med. Chem.* **2000**, *43*(14), 2664.
[25] C. A. Lipinski, F. Lombardo, B. W. Dominy, P. J. Feeney, *Adv. Drug Delivery Rev.* **1997**, *23*(1–3), 3. https://doi.org/10.1016/s0169-409x(96)00423-1
[26] P. F. Chan, V. Srikannathasan, J. Huang, H. Cui, A. P. Fosberry, M. Gu, M. M. Hann, M. Hibbs, P. Homes, K. Ingraham, J. Pizzollo, C. Shen, A. J. Shillings, C. E. Spitzfaden, R. Tanner, A. J. Theobald, R. A. Stavenger, B. D. Bax, M. N. Gwynn, *Nat. Commun.* **2015**, *6*, 10048. https://doi.org/10.1038/ncomms10048
[27] A. E. Evren, A. B. Karaduman, B. N. Sağlik, Y. Özkay, L. Yurttaş, *ACS Omega* **2023**, *8*(1), 1410. https://doi.org/10.1021/acsomega.2c06871
[28] CLSI, *Methods for dilution antimicrobial susceptibility tests for bacteria that grow aerobically; approved standard—ninth edition. CLSI document M07-A9*. Clinical and Laboratory Standards Institute, Wayne, Pennsylvania, USA **2012**.
[29] J. L. Rodriguez-Tudela, M. C. Arendrup, F. Barchiesi, J. Bille, E. Chryssanthou, M. Cuenca-Estrella, E. Dannaoui, D. W. Denning, J. P. Donnelly, F. Dromer, W. Fegeler, C. Lass-Flörl, C. Moore, M. Richardson, P. Sandven, A. Velegraki, P. Verweij, *Clin. Microbiol. Infect.* **2008**, *14*(4), 398. https://doi.org/10.1111/j.1469-0691.2007.01935.x
[30] A. Daina, O. Michielin, V. Zoete, *Sci. Rep.* **2017**, *7*(1), 42717. https://doi.org/10.1038/srep42717
[31] Schrödinger release. 2020-3: LigPrep 2020, Schrödinger, LLC, New York, NY, USA. **2020**.
[32] Schrödinger Release 2020-3, Glide, Schrödinger, LLC, New York, NY, USA. **2020**.
[33] S. Dawbaa, D. Nuha, A. E. Evren, M. Y. Cankiliç, L. Yurttaş, G. Turan, *J. Mol. Struct.* **2023**, *1282*, 135213. https://doi.org/10.1016/j.molstruc.2023.135213
[34] Schrödinger Release 2020-3, Desmond, Schrödinger, LLC, New York, NY, USA. **2020**.

SUPPORTING INFORMATION

Additional supporting information can be found online in the Supporting Information section at the end of this article.

How to cite this article: A. E. Evren, D. Nuha, S. Dawbaa, U. Kayış, Ü. D. Gül, L. Yurttaş, *Arch. Pharm.* **2025**, *358*, e2400795. https://doi.org/10.1002/ardp.202400795